

We sincerely thank the reviewers for the time and valuable comments, which have led us to a substantially improved version of the paper. We carefully considered all of these comments and revised the manuscript thoroughly. Our detailed responses to the referee's questions and comments are listed below, and the modification has been marked in the following manuscript.

Reply to Anonymous Referee #2:

The authors addressed all my issues in the response. The scientific contribution has been discussed and emphasized in the revision. The manuscript may be published after the following minor changes:

Comment 1. Line 306: "Fig. 8 shows ..." The Fig. 8 should be Figure. 8 when it comes at the beginning of a sentence. Please also revise other abbreviation according to ACP manuscript preparation guidelines.

Response:

Thanks for pointing this out. We have revised this nonstandard writing as well as other abbreviation in the full text, according to the referee's advice and ACP manuscript preparation guidelines.

Comment 2. Line 311: "The probabilities of bias by Li and MM5 within $\pm 2.5W \cdot m^{-2}$ are 32.54% and 13.49%, respectively." Spaces should be included between number and unit.

Response:

We have corrected this mistake as well as the similar problems in the full text according to the referee's kind advice.

Comment 3. Figures: Please clear the right boundary of Figure 9.

Response:

We have cleared the right boundary of Figure 9 in the revised manuscript.

Reply to Anonymous Referee #3:

The authors were very responsive and have done a lot of work to address the concerns from the reviewers. All my major questions and concerns have been well addressed in details. The paper has been significantly improved and I recommend acceptance for publication after some minor/technical revisions/corrections. Note that there are still a lot of grammar errors or typos and I may not be able to identify all of them. A thorough editing is still required.

Minor suggestions or technical corrections:

Comment 1. Abstract: Since the title mentions about the severe haze pollution, it should be identified in the abstract that the evaluation was done for haze cases.

Response:

Thanks for the referee's advice. We have changed the third sentence to "The differences of two surface layer schemes (the Li and MM5 scheme) were discussed and the performance of the two schemes focusing on a heavy haze episode was mainly evaluated based on the observed momentum and sensible heat fluxes in Jing-Jin-Ji in east China." in Lines 21-23.

Comment 2. Lines 19-21, "The pollutants prediction by atmosphere chemical model exist obvious deficiencies, which may be closely related to the uncertainties of the momentum and sensible heat fluxes calculated in the surface layer": Here "prediction", not "pollutants" , is a singular subject and hence a singular verb "exists" should be used.

Response:

The word "exist" has been changed to "exists" in Line 20.

Comment 3. Line 26, "the algorithms of universal functions": universal functions for what? Surface fluxes? Please specify.

Response:

Yes. It is universal functions for surface turbulent fluxes. So we have added "for surface turbulent fluxes" after "universal functions" in Line 27.

Comment 4. Lines 60-61, "Many international scholars verified the MOST using of field experiments": Do the authors mean "Many international scholars verified the MOST using field experiments"?

Response:

Yes. We have removed the "of" in this sentence in Line 62.

Comment 5. Line 75, "have" should be "has".

Response:

The word “have” has been changed to “has” in Line 76.

Comment 6. Lines 80-82, “The observed momentum and sensible heat flux data covering once complete haze process at Gucheng station was used to evaluate the two schemes focusing on the transition stage from unstable to stable atmospheric stratification corresponding to the PM2.5 accumulation”: “once” should be “one”; “was”: should be “were”; “evaluate” should be “evaluated”; “focusing” should be “focusing”.

Response:

We have rewritten the sentence as “The observed momentum and sensible heat flux data covering one complete haze process at Gucheng station were used to evaluate the two schemes focusing on the transition stage from unstable to stable atmospheric stratification corresponding to the PM2.5 accumulation” in Line 81-83.

Comment 7. Lines 90-91: The period “.” after the equation should be a comma “,” and “Where” should not be capitalized. Check all the other equations in which “where” is used.

Response:

We revised this mistake in Line 92-93 as well as other places where the mistake existed according to the referee’s kind advice.

Comment 8. Line 92: A comma “,” needs to be added in front of “respectively”.

Response:

We added the “,” in front of “respectively” in Line 94.

Comment 9. Line 93: The subject “they” can be omitted.

Response:

The word “They” has been omitted in Line 95.

Comment 10. Line 99: do the authors mean “from at least two levels”?

Response:

Yes. Thanks for pointing this out, and we added “from” before “at least two levels” in Line 101.

Comment 11. Line 101: “employ” should be “employs”.

Response:

We have changed the word “employ” to “employs” in Line 101.

Comment 12. Line 112: should “universe” be “universal”?

Response:

Yes. This mistake has been corrected in Line 114.

Comment 13. Line 183: add “were” before “measured”.

Response:

Thanks for pointing this out. We have added “were” before “measured” in Line 185.

Comment 14. Section 3: It is my understanding that this study focuses on the impact of the surface flux parameterization on air pollution modeling. Therefore, the haze pollution case(s) or episode(s) should also be briefly described in this section.

Response:

We appreciate the referee’s suggestion. Our study indeed focuses on the impact of the surface flux parameterization on air pollution modeling, but there are also some analyses and evaluation on non-pollution period in Section 4. Therefore, we described the haze pollution case after the whole discussion in Section 4, which can make the organization clearer.

Comment 15. Line 370: “results in” should be “result in”.

Response:

We have revised this mistake in Line 374.

We thoroughly checked the full text according to the referees’ suggestions and ACP manuscript preparation guidelines, and all revision details can be seen in the marked-up manuscript version below.

~~The e~~Evaluating study of the momentum and heat exchange process of two surface layer schemes during ~~the~~ severe haze pollution in Jing-Jin-Ji in east China

Yue Peng^{1,2}, Hong Wang^{1,2}, Yubin Li³, Changwei Liu³, Tianliang Zhao², Xiaoye Zhang¹, Zhiqiu Gao^{3,4}, Tong Jiang⁵, Huizheng Che¹, Meng Zhang⁶

¹ State Key Laboratory of Severe Weather/Institute of Atmospheric Composition, Chinese Academy of Meteorological Sciences (CMAS), Beijing 100081, China

² Collaborative Innovation Center on Forecast and Evaluation of Meteorological Disasters/Key Laboratory for Aerosol-Cloud-Precipitation of China Meteorological Administration, Nanjing University of Information Science and Technology, Nanjing 210044, China

³ Key Laboratory of Meteorological Disaster of Ministry of Education/Collaborative Innovation Center on Forecast and Evaluation of Meteorological Disasters, School of Remote Sensing and Geomatics Engineering, Nanjing University of Information Science and Technology, Nanjing 210044, China

⁴ State Key Laboratory of Atmospheric Boundary Layer Physics and Atmospheric Chemistry, Institute of Atmospheric Physics, Chinese Academy of Sciences, Beijing 100029, China

⁵ National Climate Center, China Meteorological Administration, Beijing 100081, China

⁶ Beijing Meteorological Service, Beijing 100089, China

Correspondence to: Hong Wang (wangh@cma.gov.cn)

Abstract. The turbulent flux parameterization schemes in ~~the~~ surface layer are crucial for air pollution modeling. ~~The~~ ~~p~~Pollutants prediction by atmosphere chemical model exists obvious deficiencies, which may be closely related to the uncertainties of the momentum and sensible heat fluxes calculated in the surface layer. The differences of two surface layer schemes (the Li and MM5 scheme) were discussed and the performance of the two schemes ~~focusing on a heavy haze episode~~ was ~~mainly~~ -evaluated based on the observed momentum and sensible heat fluxes in Jing-Jin-Ji in east China. The results showed that the aerodynamic roughness length z_{0m} and the thermal roughness length z_{0h} play an ~~important~~major role in the flux calculation. Compared with the Li scheme, ignoring the difference between the two in the MM5 scheme induced a great error in the calculation of sensible heat flux (e.g., the error was 54% at Gucheng station). Besides the roughness lengths, the algorithms of universal functions ~~for surface turbulent fluxes~~ as well as the roughness sublayer also resulted in certain errors in the MM5 scheme. In addition, ~~the~~magnitudes of z_{0m} and z_{0h} ~~has~~ve significant influence on the two schemes. The large z_{0m} and z_{0m}/z_{0h} in megacity with rough surface (e.g., Beijing) resulted in much larger differences of momentum and sensible heat fluxes by Li and MM5, compared with the small z_{0m} and z_{0m}/z_{0h} in suburban area with smooth surface (e.g., Gucheng). The Li scheme better characterized the evolution of atmospheric stratification than the MM5 scheme in general, especially for the transition stage from unstable to stable atmospheric stratification corresponding to the PM_{2.5} accumulation. The bias of momentum and sensible heat fluxes from Li were lower about 38% and 43% respectively than those from MM5 during this stage. This study indicates the superiority of the Li

scheme in the describing of the regional atmospheric stratification, and also suggests the improving possibility of severe haze prediction in Jing-Jin-Ji in east China by coupling it into the atmosphere chemical model online.

Key words: surface layer; turbulent flux parameterization; roughness length; numerical modeling; air pollution

1 Introduction

Adequate air quality modeling relies on accurate simulations of meteorological conditions, especially in the planetary boundary layer (PBL) (Hu et al., 2010; Cheng et al., 2012; Xie et al., 2012). The PBL is closely-tightly coupled to the earth's surface by turbulent exchange processes. As the bottom layer of PBL, the surface layer (SL) reflects the surface state by calculating momentum, heat, water vapor and other fluxes, and influences the atmospheric structure by turbulent transport process. Many studies have illustrated the important roles of meteorological factors in the SL in the formation of air pollution. They demonstrated that weak wind speed, high relative humidity (RH) and strong temperature inversion are favorable for the haze concentrating (Zhang et al., 2014; Yang et al., 2015; Liu et al., 2017; Zhong et al., 2017). The strong stable stratification and weak turbulent are mainly responsible for many haze events. The relationship between flux and atmospheric profile in the atmospheric surface layer is a keycritical factor for air pollution diffusion, especially under stable stratification conditions (Li et al., 2017). However, the study of stable boundary layer still has some uncertainties due to the poor description of surface turbulent motion. The simulating study on a severe haze in east China by the Weather Research and Forecasting/Chemistry (WRF-Chem) model concluded that there is lower ability of current PBL schemes in distinguishing the diffusion between haze days under stable condition and clean days under unstable condition (Li et al., 2016a). Another study (Vautard et al. 2012) on mesoscale meteorological models also pointed out a systematic overestimation of near-surface wind speed in a stable boundary layer and its possible contribution to the underestimation of the PM_{2.5} pollution. In addition, atmospheric conditions in both the PBL and upper layers are stronghighly dependent on the turbulent fluxes which are computed in the SL (Ban et al., 2010). Flux parameterization in the SL plays an important role in studies of the hydrological cycle and weather prediction (Yang et al., 2001; Li, 2014). An adequate SL scheme is crucial to provide an accurate atmospheric evolution by numerical models (Jiménez et al., 2012) and hence it may introduce important significant impacts on air pollution simulation.

The bulk aerodynamic formulation based on Monin-Obukhov similarity theory (hereinafter MOST, Monin and Obukhov, 1954) is usually employed to calculate surface fluxes in numerical models. Turbulent fluxes are parameterized by wind, temperature, humidity in the lowest layer in the model and temperature and humidity at the in-surface. Many international scholars verified the MOST using of-field experiments and then proposed the universal functions, the commonly used of which is Businger-Dyer (BD) equation (Businger, 1966; Dyer, 1967). With the development of observation technology, the coefficients in the BD equation have been further modified (Paulson, 1970; Webb, 1970;

65 Businger et al., 1971; Dyer, 1974; Högström, 1996). In addition to the BD equation, some other schemes have been put
66 forward and they performed better especially for ~~the~~ strongly stable stratification (Holtslag and De Bruin, 1988; Beljaars and
67 Holtslag, 1991; Cheng and Brutsaert, 2005). The schemes can be divided into two types according to the
68 computing characteristics. One type is called as iterative algorithm (Paulson, 1970; Businger et al., 1971; Dyer, 1974;
69 Högström, 1996; Beljaars and Holtslag, 1991), and it keeps the MOST completely with less approximation so that the results
70 can be more precise. However, it needs to take much more steps to converge and hence the CPU time is consuming which
71 reduces the computational efficiency of modeling (Louis, 1979; Li et al., 2014); The other one is called as non-iterative
72 algorithm (Louis et al., 1982; Launiainen, 1995; Wang et al., 2002; Wouters et al., 2012). There is no ~~requirement~~~~need~~ for
73 loop iteration in the calculation due to the approximate treatment. This algorithm is much simpler and less CPU
74 time-consuming, but the results are based on the loss of the calculation accuracy.

75 A new non-iterative scheme proposed by Li et al. (2014; 2015, Li hereinafter) speeds up effectively under a higher
76 accuracy compared with some classic iterative computation. It is remarkable that this new scheme just ~~have~~~~has~~ been
77 theoretically evaluated and it has never been applied in any models. Haze pollution occurs frequently in recent years in east
78 China. The concentration of PM_{2.5} may reach up to 1000 $\mu\text{g}\cdot\text{m}^{-3}$ in the Beijing-Tianjin-Hebei (Jing-Jin-Ji) region in
79 winter (Wang et al., 2014) while it was generally underestiamated by current air quality models (Zhang et al., 2015; Li et al.,
80 2016a; Liu et al., 2017). The Li and another classic SL scheme (Zhang and Anthes, 1982, MM5 hereinafter) are compared in
81 details in this study. The observed momentum and sensible heat flux data covering ~~one~~ complete haze process at Gucheng
82 station ~~was~~~~were~~ used to evaluate the two schemes focus~~ing~~ on the transition stage from unstable to stable atmospheric
83 stratification corresponding to the PM_{2.5} accumulation. The evaluation is in the view of both local and regional scales. This
84 offline study may provide the prerequisite for the online coupling the Li scheme into atmosphere chemical model in the
85 future.

86 2 Theory

87 The definition of ~~the~~ momentum and sensible heat flux as well as the detailed algorithms of the Li and MM5 schemes
88 are introduced in this section.

89 2.1 Introduction of the momentum and sensible heat flux

90 The turbulent fluxes from ground surface are defined as follows:

$$91 \tau = \rho u_*^2, \quad (1a)$$

$$92 H = -\rho c_p u_* \theta_* \quad (1b)$$

93 ~~W~~where τ is the momentum flux, H is the sensible heat flux, ρ is the air density, c_p is the specific heat capacity at
94 constant pressure. u_* and θ_* are the friction velocity and the temperature scale, respectively, and they represent the

带格式的: 缩进: 首行缩进: 0 字符

intensity of the vertical turbulent flux transport and they are approximately independent on height in the SL.

Both the Li and MM5 schemes are calculated with bulk flux parameterization. As an important dimensionless parameter related to the stability, the bulk Richardson number Ri_B is defined as

$$Ri_B = \frac{gz(\theta - \theta_g)}{\theta u^2} \quad (2)$$

Where g is the acceleration of gravity, z is the reference height which is the lowest level in the model, θ is the mean potential temperature at height z , θ_g is the surface radiometric potential temperature, u is the mean wind speed at height z .

Thus, Ri_B can be computed through meteorological variables from at least two levels.

2.2 The Li scheme

This new scheme employs non-iterative algorithm to compute the surface fluxes. Its basic idea is to parameterize the stability parameter ζ directly with Ri_B and roughness lengths (z_{0m} and z_{0h}). Specifically, bulk transfer coefficients of the momentum and sensible heat fluxes (C_M and C_H) are expressed as

$$C_M = \frac{u_*^2}{u^2} = \frac{\tau}{\rho u^2} \quad (3a)$$

$$C_H = \frac{u_* \theta_*}{u(\theta - \theta_g)} = -\frac{H}{\rho c_p u(\theta - \theta_g)} \quad (3b)$$

Based on MOST and considering the roughness sublayer (RSL) effect at the same time, the relationships between the bulk transfer coefficients and the profile functions corresponding to wind and potential temperature are usually expressed as

$$C_M = \frac{k^2}{\left[\ln \frac{z}{z_{0m}} - \psi_M \left(\frac{z}{L} \right) + \psi_M \left(\frac{z_{0m}}{L} \right) + \psi_M^* \left(\frac{z}{z_*}, \frac{z_*}{L} \right) \right]^2} \quad (4a)$$

$$C_H = \frac{k^2}{R \left[\ln \frac{z}{z_{0m}} - \psi_M \left(\frac{z}{L} \right) + \psi_M \left(\frac{z_{0m}}{L} \right) + \psi_M^* \left(\frac{z}{z_*}, \frac{z_*}{L} \right) \right] \left[\ln \frac{z}{z_{0h}} - \psi_H \left(\frac{z}{L} \right) + \psi_H \left(\frac{z_{0h}}{L} \right) + \psi_H^* \left(\frac{z}{z_*}, \frac{z_*}{L} \right) \right]} \quad (4b)$$

Where k is the von Kármán constant which is 0.4 in both two schemes, R is the Prandtl number which is 1.0 in the two schemes, z_{0m} and z_{0h} are the aerodynamic roughness length and the thermal roughness length, respectively. ψ_M and ψ_H are the integrated stability functions for momentum and sensible heat, respectively, which are also called universal functions. L is the Obukhov length ($\zeta = \frac{z}{L}$), ψ_M^* and ψ_H^* are the correction functions accounting for RSL effect, z_* is the RSL height. It is clear to see that the calculation of the momentum and sensible heat fluxes requires C_M and C_H (or u_* and θ_*), and there are 3 key points to get them:

1. z_{0m} and z_{0h} . z_{0m} and z_{0h} are two key parameters in the bulk transfer equations. Their definitions and influence will be discussed in Sect. 4.1. Note that both z_{0m} and z_{0h} are taken into account by the Li scheme. In other words, the Li scheme distinguishes these two principal important surface parameters effectively as they generate from different mechanisms.

2. ζ . The determination of ζ is the most crucial problem for the Li scheme. In fact, this new scheme consists of includes two parts. The first part was proposed for atmospheric stable stratification condition (Li et al., 2014), and the

带格式的: 缩进: 首行缩进: 0 字符

带格式的: 缩进: 首行缩进: 0 字符

124 second part then extended the scheme to unstable condition (Li et al., 2015). For stable condition, the calculation
 125 procedure for a given group of Ri_B , z_{0m} and z_{0h} is the following: (1) find the region according to z_{0m} and z_{0h} ; (2)
 126 find the section according to the region and Ri_B with Eq. (5) and given coefficients; (3) calculate ζ using Eq. (6) and
 127 given coefficients.

$$128 \quad Ri_{Bcp} = \sum C_{mn} (\log L_{0M})^m (L_{0H} - L_{0M})^n, \quad (5)$$

$$129 \quad \zeta = Ri_B \sum C_{ijk} Ri_B^i L_{0M}^j (L_{0H} - L_{0M})^k, \quad (6)$$

130 **W**where C_{mn} and C_{ijk} are the coefficients in Tables in Li et al. (2014). $L_{0M} = \ln \frac{z}{z_{0m}}$, $L_{0H} = \ln \frac{z}{z_{0h}}$. $m, n = 0, 1, 2,$
 131 and $m + n \leq 3$; $i, j, k = 0, 1, 2, 3$, and $i + j + k \leq 4$. Similarly, for unstable condition, eight regions are divided
 132 according to the method from Li et al. (2015). For each of the regions, ζ is carried out by following:

$$133 \quad \zeta = Ri_B \frac{L_{0M}^2}{L_{0H}} \sum C_{ijk} \left(\frac{-Ri_B}{1-Ri_B} \right)^i L_{0M}^{-j} L_{0H}^{-k}, \quad (7)$$

134 **W**where C_{ijk} is listed in Li et al. (2016b), and $i = 0, 1$; $j, k = 0, 1, 2, 3$; $i + j + k \leq 4$.

135 3. Universal function. It is also a key factor in flux calculation. The form of universal function here is adopted from
 136 Cheng and Brutsaert (2005) under the stable condition (Eqs. (8a), (8b)) and it is adopted from Paulson (1970) under the
 137 unstable condition (Eqs. (9a), (9b)):

$$138 \quad \psi_M(\zeta) = -a \ln \left[\zeta + (1 + \zeta^b)^{\frac{1}{b}} \right], \quad \zeta > 0 \text{ (stable)}, \quad (8a)$$

$$139 \quad \psi_H(\zeta) = -c \ln \left[\zeta + (1 + \zeta^d)^{\frac{1}{d}} \right], \quad \zeta > 0 \text{ (stable)}, \quad (8b)$$

$$140 \quad \psi_M(\zeta) = 2 \ln \frac{1+x}{2} + \ln \frac{1+x^2}{2} - 2 \arctan(x) + \frac{\pi}{2}, \quad \zeta < 0 \text{ (unstable)}, \quad (9a)$$

$$141 \quad \psi_H(\zeta) = 2 \ln \frac{1+y}{2}, \quad \zeta < 0 \text{ (unstable)}. \quad (9b)$$

142 **W**where $a = 6.1$, $b = 2.5$, $c = 5.3$, $d = 1.1$, $x = (1 - 16\zeta)^{1/4}$, $y = (1 - 16\zeta)^{1/2}$.

143 In addition, the RSL effect is taken into account in the Li scheme. The definitions and influence of RSL will also be
 144 discussed in Sect. 4.1. De Ridder (2010) proposed the expression of ψ_M^* and ψ_H^* :

$$145 \quad \psi_M^* \left(\zeta, \frac{z}{z_*} \right) = \phi_M \left[\left(1 + \frac{v}{\mu_M z / z_*} \right) \zeta \right] \frac{1}{\lambda} \ln \left(1 + \frac{\lambda}{\mu_M z / z_*} \right) e^{-\mu_M z / z_*}, \quad (10a)$$

$$146 \quad \psi_H^* \left(\zeta, \frac{z}{z_*} \right) = \phi_H \left[\left(1 + \frac{v}{\mu_H z / z_*} \right) \zeta \right] \frac{1}{\lambda} \ln \left(1 + \frac{\lambda}{\mu_H z / z_*} \right) e^{-\mu_H z / z_*}, \quad (10b)$$

147 **W**where $v = 0.5$, $\mu_M = 2.59$, $\mu_H = 0.95$, $z_* = 16.7 z_{0m}$, $\lambda = 1.5$. ϕ_M and ϕ_H are universal functions before
 148 integration. Here, set $\chi_M = 1 + \frac{v}{\mu_M z / z_*}$, $\chi_H = 1 + \frac{v}{\mu_H z / z_*}$:

$$149 \quad \phi_M(\chi_M \zeta) = 1 + a \frac{\chi_M \zeta + (\chi_M \zeta)^b [1 + (\chi_M \zeta)^b]^{\frac{1-b}{b}}}{\chi_M \zeta + [1 + (\chi_M \zeta)^b]^{\frac{1}{b}}}, \quad \zeta > 0 \text{ (stable)}, \quad (11a)$$

带格式的: 缩进: 首行缩进: 0 字符

带格式的: 缩进: 左侧: 0 厘米, 首行缩进: 0 字符

带格式的: 缩进: 左侧: 0 厘米, 首行缩进: 0 字符

带格式的: 缩进: 首行缩进: 0 字符

$$\phi_H(\chi_H\zeta) = 1 + c \frac{\chi_H\zeta + (\chi_H\zeta)^d [1 + (\chi_H\zeta)^d]^{\frac{1-d}{d}}}{\chi_H\zeta + [1 + (\chi_H\zeta)^d]^{\frac{1}{d}}}, \quad \zeta > 0 \text{ (stable)}, \quad (11b)$$

$$\phi_M(\chi_M\zeta) = (1 - 16\chi_M\zeta)^{-1/4}, \quad \zeta < 0 \text{ (unstable)}, \quad (12a)$$

$$\phi_H(\chi_H\zeta) = (1 - 16\chi_H\zeta)^{-1/2}, \quad \zeta < 0 \text{ (unstable)}. \quad (12b)$$

2.3 The MM5 scheme

The MM5 scheme is a classic one which is widely applied in modeling investigation (Hu et al., 2010; Wang et al., 2015a, b; Tymvios et al., 2017). This scheme does not distinguish z_{0h} from z_{0m} , thus the roughness length here is expressed as z_0 . For unstable condition, the function forms are given by Eqs. (16a) and (16b) following Paulson (1970), and for stable condition, the atmospheric stratification conditions are subdivided into three cases according to Zhang and Anthes (1982) and the function forms are given by Eqs. (13), (14), and (15).

(1) Strongly stable condition ($Ri_B \geq 0.2$):

$$\psi_M = \psi_H = -10 \ln \frac{z}{z_0}. \quad (13)$$

(2) Weakly stable condition ($0 < Ri_B < 0.2$):

$$\psi_M = \psi_H = -5 \left(\frac{Ri_B}{1.1 - 5Ri_B} \right) \ln \frac{z}{z_0}. \quad (14)$$

(3) Neutral condition ($Ri_B = 0$):

$$\psi_M = \psi_H = 0. \quad (15)$$

(4) Unstable condition ($Ri_B < 0$):

$$\psi_M = 2 \ln \frac{1+x}{2} + \ln \frac{1+x^2}{2} - 2 \arctan(x) + \frac{\pi}{2}, \quad (16a)$$

$$\psi_H = 2 \ln \frac{1+y}{2}, \quad (16b)$$

where $x = (1 - 16\zeta)^{1/4}$, $y = (1 - 16\zeta)^{1/2}$.

This scheme calculates turbulent fluxes of the momentum and sensible heat with u_* and θ_* . In order to avoid the huge difference of u_* through the two computations, u_* is arithmetically averaged with its previous value with-by Eq. (17), and a lower limit of $u_* = 0.1$ m/s is imposed to prevent the heat flux from being zero under very stable conditions. According to the profile functions of wind and temperature near the ground, θ_* then is deduced by Eq. (18).

$$u_* = \frac{1}{2} \left(u_* + \frac{ku}{\ln \frac{z}{z_{0m}} - \psi_M} \right), \quad (17)$$

$$\theta_* = \frac{k(\theta - \theta_R)}{R[\ln \frac{z}{z_{0h}} - \psi_H]}. \quad (18)$$

The calculation procedure of the Li scheme is the following: (1) determine Ri_B , z_{0m} and z_{0h} according to the observation data; (2) calculate ζ with Ri_B , z_{0m} and z_{0h} ; (3) calculate the momentum and sensible heat fluxes under different conditions. The MM5 scheme is summarized as follows: (1) determine the universal functions according to the

178 values of Ri_B and z_0 ; (2) calculate the u_* and θ_* with the meteorological variables and flux data; (3) derive the turbulent
179 fluxes. Compared with other non-iterative schemes including MM5, the Li scheme can be applied to the full range of
180 roughness status $10 \leq \frac{z}{z_{om}} \leq 10^5$ and $-0.5 \leq \ln \frac{z_{om}}{z_{oh}} \leq 30$ under whole conditions $-5 \leq Ri_B \leq 2.5$. In addition, there are
181 three obvious differences between the Li and MM5 schemes: (1) Li distinguishes z_{oh} from z_{om} but MM5 does not
182 distinguish them; (2) the two schemes apply different universal functions under stable condition; (3) Li considers the RSL
183 effect while MM5 ignores it.

184 **3 Observational data and methods**

185 The observational fluxes used in this study were measured at Gucheng station from December 1, 2016 to January 9,
186 2017. Gucheng station (115.40 °E, 39.08 °N) is located at Gucheng County, Baoding, Hebei province and it is about 110km
187 southwest of Beijing (Fig. 1a). This station has a farmland site where rice is planted in summer and wheat in winter. The
188 surroundings are mainly farmland and scattered villages (Fig. 1b). At Gucheng station, the momentum and sensible heat
189 fluxes near the surface were measured by the eddy correlation flux measurement system. The system is mainly composed of
190 a sonic anemometer (CSAT3) and a gas analyzer (LI-7500). They are set up at 4_m height above the surface ground. The
191 measured fluxes are used to evaluate the two schemes as well as estimate the roughness lengths. The measured
192 meteorological variables including wind speed and direction, temperature, humidity, pressure, radiation are used-utilized to
193 calculate the momentum and sensible heat fluxes both in the Li and MM5 schemes. Note the observed meteorological data
194 were from Gucheng station and national basic automatic weather stations in Jing-Jin-Ji in east China, respectively. Hourly
195 surface PM_{2.5} mass concentration in Baoding and Beijing from China National Environmental Monitoring Centre
196 (<http://www.cnemc.cn/>) were also used in this paper.

197 **3.1 Data processing**

198 To obtain accurate flux data, quality control has been performed for the observational data, including: (1) eliminate the
199 outliers and the data in rainy days; (2) double rotation and WPL correction (Webb et al., 1980); (3) omit the dataset when the
200 wind speed is less than $0.5 \text{ m} \cdot \text{s}^{-1}$. In addition, the wind field especially the wind direction has a great impact on the value of
201 z_{om} , so it is necessary to understand the situation at Gucheng station. Figure 2 shows the distribution frequency of wind
202 speed and wind direction at Gucheng during the observation (December 1, 2016 ~ January 9, 2017). The wind speed is stable
203 during this period and the maximum is no more than $5 \text{ m} \cdot \text{s}^{-1}$ and most of them are about $1 \sim 2 \text{ m} \cdot \text{s}^{-1}$. The wind direction is
204 relatively uniform except for the southeast wind (135°).

205 **3.2 Determination of surface skin temperature**

206 The surface skin temperature at Gucheng station is calculated from the radiation data by the following formula:

带格式的：上标

带格式的：上标

带格式的：上标

带格式的：字体：Times New Roman

$$R_{lw}^{\uparrow} = (1 - \varepsilon_s)R_{lw}^{\downarrow} + \varepsilon_s \sigma T_g^4, \quad (19)$$

where R_{lw}^{\uparrow} and R_{lw}^{\downarrow} are the surface upward longwave radiation and long wave radiation incident on the surface, respectively. σ is the Stephen Boltzmann constant, $\sigma = 5.67 \times 10^{-8} \text{ W m}^{-2} \text{ K}^{-4}$. T_g is the surface skin temperature, ε_s is the surface emissivity which is the prerequisite for calculating T_g . Many researches estimated ε_s and the range of the values is always $0.9 \sim 1$ (Stewart et al., 1994; Verhoef et al., 1997). According to the semi-empirical method in Yang et al. (2008), ε_s is estimated when the RMSE is minimal. In this paper, the Li and MM5 schemes were used to estimate the ε_s value (as shown in Fig. 3). It is clear that the ε_s value corresponding to the minimum RMSE is not very sensitive to the choice of two schemes. When ε_s is 1, the RMSE has the minimum value. Thus, this experiment takes 1 as the optimal value of ε_s .

3.3 Determination of roughness length z_{0m} (z_{0h})

Using the observed momentum and sensible heat fluxes and the meteorological variables including wind speed, temperature, humidity and pressure after quality control at Gucheng station, z_{0m} and z_{0h} were derived by from Eqs. (20a) and (20b) following Yang et al. (2003) and Sicart et al. (2014).

$$\frac{u_*}{u} = \frac{k}{\ln \frac{z}{z_{0m}} - \psi_M}, \quad (20a)$$

$$\frac{\theta_*}{(\theta - \theta_g)} = \frac{k}{R \left[\ln \frac{z}{z_{0h}} - \psi_H \right]}. \quad (20b)$$

During the observation period, the crops stopped growing and the height did not exceed 0.1 m, so the zero-plane displacement height was ignored hence the reference height z was taken as 4m. The observation time was too short (about 1 month) to consider the effect of seasonal variations on roughness lengths. Thus, z_{0m} and z_{0h} were assumed as two fixed values. Based on the variables and formulae mentioned above, the roughness lengths at Gucheng are derived: $z_{0m} = 0.0419 \text{ m}$, $z_{0h} = 0.0042 \text{ m}$.

4 Results and discussion

The RSL, roughness length and their influence on the calculation of turbulent flux are discussed in detail in this section. The Li and MM5 schemes are offline tested and evaluated during the haze pollution from December 13 to 23, 2016.

4.1 The influence of RSL and roughness length on the calculation of turbulent flux

The RSL is usually defined as the region where the flow is influenced by the individual roughness elements as reflected by the spatial inhomogeneity of the mean flow (Florens et al., 2013). In the RSL, turbulence is strongly affected by individual roughness elements, and the standard MOST is no longer valid (Simpson et al., 1998). Therefore, it is necessary to consider the RSL effect in the calculation of turbulent fluxes, especially for the rough terrain such as forest or large cities.

235 z_{0m} is defined as the height at which the extrapolated wind speed following the similarity theory vanishes. It is mainly
 236 determined by land-cover type and canopy height after excluding large obstructions. In models, z_{0m} is always based on the
 237 look-up table which is related to land-cover types. In this study, z_{0m} was simply classified based on the research of Stull
 238 (1988) listed in Table 1. It can be seen in Table 1 that the rougher underlying surface corresponds to the larger value of z_{0m} .
 239 z_{0h} is the height at which the extrapolated air temperature is identical to the surface skin temperature. Some early
 240 researchers assumed that z_{0m} was equal to z_{0h} (Louis, 1979; Louis et al., 1982). However, the assumption is not
 241 applicable in reality because z_{0m} and z_{0h} have different physical meanings. Different treatment of z_{0m} and z_{0h} may
 242 introduce considerable changes in the surface flux calculation (Launiainen, 1995; Kot and Song, 1998; Anurose and
 243 Subrahmanyam, 2013). Many studies removed the assumption that z_{0m} was equal to z_{0h} and made the schemes more
 244 applicable in the situation that z_{0m} was not equal to z_{0h} or the ratio of z_{0m} to z_{0h} was much large (Wouters et al., 2012;
 245 Li et al., 2014; Li et al., 2015). Some field experiments even indicated the ratio z_{0m}/z_{0h} has a diurnal variation (Sun, 1999;
 246 Yang, 2003; Yang, 2008). In this study, we make the common assumption that the ratio z_{0m}/z_{0h} is a constant.

247 Considering the lowest level in mesoscale models is usually about 10m, $z = 10$ m is set as the reference height. The
 248 range of Ri_B is set according to Louis82 (Louis et al., 1982) in the following discussion. Firstly, the effects of different
 249 land-cover types (different z_{0m} values) and RSL on flux calculation were discussed. Set $z_{0m} = z_{0h}$, corresponding to four
 250 cases: $z_{0m} = 1, 0.5, 0.05, 0.001$ m. These cases correspond to large cities, forests, agricultural fields and wide water surface,
 251 respectively. Figure 4 shows the relationship between $C_M(C_H)$ and Ri_B for different z_{0m} values and treatment of RSL.
 252 It can be seen that both RSL and z_{0m} have impacts on C_M and C_H . Ignoring the RSL effect results in larger C_M and C_H ,
 253 compared with the results of original scheme considering the RSL. The difference induced by RSL is obvious-evident only
 254 under the rough surface. For example, the difference under $z_{0m} = 1$ is obviously greater than other z_{0m} settings, and when
 255 z_{0m} is reduced to 0.05 or less, the RSL has little effect. Furthermore, the RSL contributes more to sensible heat transfer than
 256 to momentum transfer under the same setting of z_{0m} . The effects of different land-cover types on C_M and C_H are much
 257 more significant compared with RSL. The rougher the surface is (corresponding to the larger z_{0m} value), the larger the C_M
 258 (C_H) is. In addition, there is a corresponding relationship between $C_M(C_H)$ and stability. The more unstable the atmosphere
 259 is, the larger difference the value of $C_M(C_H)$ is and vice versa. Once Ri_B exceeds the critical value (generally 0.2~0.25),
 260 the transfer coefficients decline sharply but still above 0.

261 Secondly, the effects of difference between z_{0m} and z_{0h} as well as RSL on flux calculation are discussed. The
 262 relationship between z_{0m} and z_{0h} can be expressed as $kB^{-1} = \ln \frac{z_{0m}}{z_{0h}}$. Over the sea, z_{0m} is comparable to z_{0h} ; over the
 263 uniform vegetation surface (grassland, farmland, woodland), kB^{-1} is about 2 ($z_{0m}/z_{0h} \approx 10$) (Garratt and Hicks, 1973;
 264 Garratt, 1978; Garratt and Francey, 1978), which coincides with our results in Gucheng ($z_{0m} = 0.0419$ m, $z_{0h} =$
 265 0.0042 m); over the surface with bluff roughness elements, the kB^{-1} value may be very large. For example, in some large

266 cities, kB^{-1} is even up to 30 ($z_{0m}/z_{0h} \approx 10^{13}$) (Sugawara and Narita, 2009). Therefore, the ratio z_{0m}/z_{0h} varies over a
267 wide range. [FigureFig- 5](#) shows the relationship between $C_M(C_H)$ and Ri_B for different treatment of z_{0m}/z_{0h} . Set $z_{0m} =$
268 1 as a large city case, $z_{0h}=1, 0.01, 10^{-4}, 10^{-6}$ m, and the large differences derived from the different ratios are displayed in
269 Fig. 5. The similar RSL effect can be found compared with Fig. 4. The differences induced by RSL are more obvious than
270 that in Fig. 4. The different treatment of ratio z_{0m}/z_{0h} has great impact on turbulent flux transfer, particularly for sensible
271 heat transfer. It seems evident that when z_{0h} is not equal to z_{0m} ($z_{0m}/z_{0h}=100 \sim 10^6$), the calculated C_H is much small
272 compared to the treatment that z_{0h} is equal to z_{0m} ($z_{0m}/z_{0h}=1$). In addition, $C_M(C_H)$ decreases with the increase of
273 stability, and they decrease much slower when z_{0h} is not equal to z_{0m} .

274

275 4.2 Comparison of momentum and sensible heat fluxes calculated by the two schemes

276 Using the obtained roughness lengths and the observations, the momentum and sensible heat flux were calculated by the
277 Li and MM5 schemes. Firstly, z_{0m} and z_{0h} were set as 0.0419 and 0.0042 respectively in the Li scheme, z_0 was equal to
278 z_{0m} in the MM5 scheme to calculate the momentum and sensible heat fluxes and the results are shown in Figs. 6a and 6b. It
279 can be seen that compared with MM5, Li performs better with higher regression coefficient and determination coefficient.
280 For the momentum fluxes, the regression coefficient by Li is 0.6795 and that by MM5 is 0.5598, indicating that the error of
281 Li is 12_% lower than that of MM5. For sensible heat fluxes, the regression coefficient by Li is 0.7967 and that by MM5 is
282 1.7994. The latter is much larger than 1, that is, the MM5 scheme obviously overestimates the sensible heat due to it does not
283 distinguish z_{0h} from z_{0m} . Then, make z_0 equal to 0.0042 in the MM5 scheme to re-calculate the sensible heat fluxes as
284 shown in Fig. 6c. It can be seen the result has a great improvement after modifying z_0 value and the regression coefficient
285 by MM5 is 0.7363, indicating that the error was reduced by 54_% after considering the z_{0h} effect. The result indicates that
286 z_{0h} plays a [keycritical](#) role in both the SL scheme and the sensible heat flux (Chen and Zhang, 2009; Chen et al., 2011).
287 However, the error caused by Li is still 6_% lower than that by MM5. This illustrates that in addition to the effect of
288 roughness lengths, the algorithm of the Li scheme itself is more reasonable than that of MM5 scheme.

289 4.3 The specific performance of the two schemes in the severe haze pollution

290 There were two obvious pollution processes during this observation period and one occurred during December 13 to 23,
291 2016. [FigureFig- 7](#) shows the variations of hourly observed $PM_{2.5}$ concentration as well as the momentum and sensible heat
292 fluxes calculated by the Li and MM5 schemes at Gucheng station in this process. For the research purpose significance, only
293 the daytime (from 8:00 a.m. to 20:00 p.m.) was taken into account. Note in MM5, z_0 was 0.0419 when calculate
294 momentum fluxes and it was 0.0042 when calculate sensible heat fluxes. As shown in Fig. 7, the calculated results of
295 momentum and sensible heat fluxes for the two schemes are generally consistent with the trend of the observations.

296 Specifically, for the momentum fluxes (Fig. 7a), the results of two schemes have little difference when the values of
297 observed momentum fluxes are large or at the peak. When the observed momentum fluxes are small, the Li scheme results
298 are close to or less than the observations, while the MM5 scheme results are always higher than observations because of the
299 limit of $u_* = 0.1$ in this scheme. For the sensible heat fluxes (Fig. 7b), MM5 results are always lower while Li results are
300 closer to observations especially when the observed values are small. Furthermore, according to the evolution of $PM_{2.5}$
301 concentration, this haze event was then divided into three stages: the clear stage (stage 1: 13~14), the transition stage (stage 2:
302 16~18) and the maintenance stage (stage 3: 21~22). As shown in Fig. 7, in the clear stage (stage 1), the atmospheric
303 stratification is unstable, $PM_{2.5}$ concentration is low and there is a strong flux transport in the SL, the corresponding
304 observations of the momentum and sensible heat fluxes are relatively high and they vary greatly. In the transition stage (stage
305 2), the atmosphere is changing from unstable to stable corresponding to hazes formation, the momentum and sensible heat
306 fluxes gradually decreases and the daily variation also decreases. In the maintenance stage (stage 3), the atmospheric
307 stratification is very stable, and flux transport in the SL is weak, both the momentum and sensible heat fluxes are at a low
308 level. It can be seen that the Li results are generally closer to the observations compared with MM5 results in all three stages.

309 ~~Figure~~Fig. 8 shows the probability distribution functions (PDF) of the difference of momentum fluxes (Figs. 8a, 8c, 8e,
310 8g) and sensible heat fluxes (Figs. 8b, 8d, 8f, 8h) calculated by using the Li and MM5 schemes in different stages at
311 Gucheng station. In the whole pollution process, for the momentum fluxes (Fig. 8a), the PDF of the difference by Li tends to
312 cluster in a narrower range centered by 0, and the probability within $\pm 0.005 N \cdot m^{-2}$ is 46.82%, while this value by MM5 falls
313 to 23.02%. For the sensible heat fluxes (Fig. 8b), the PDF of the difference by Li is also more concentrated around 0 than
314 that by MM5. The probabilities of bias by Li and MM5 within $\pm 2.5 W \cdot m^{-2}$ are 32.54% and 13.49%, respectively. In stage 1,
315 for the momentum fluxes (Fig. 8c), the probability of bias by Li within $\pm 0.005 N \cdot m^{-2}$ is 38.09%. The bias of MM5 mainly
316 concentrates larger than 0, and the probability within $\pm 0.005 N \cdot m^{-2}$ is 14.29%. For the sensible heat fluxes (Fig. 8d), the
317 probability of Li bias within $\pm 2.5 W \cdot m^{-2}$ is 38.09%, the same as momentum fluxes. The bias of MM5 mainly concentrates
318 less than 0, and the probability within $\pm 2.5 W \cdot m^{-2}$ is 9.52%. In stage 2, the differences between the two schemes are more
319 obvious. The momentum and sensible heat fluxes bias by Li is the most concentrated around 0 in all cases, while the
320 distribution of bias by MM5 is similar to that in stage 1. Specifically, for the momentum fluxes (Fig. 8e), the probabilities of
321 bias by Li and MM5 within $\pm 0.005 N \cdot m^{-2}$ are 56.25% and 25.00%. For the sensible heat fluxes (Fig. 8f), the probabilities
322 of bias by Li and MM5 within $\pm 2.5 W \cdot m^{-2}$ are 40.62% and 6.25%. In stage 3, the difference between two schemes is small.
323 For the momentum fluxes (Fig. 8g), the probabilities of bias by Li and MM5 within $\pm 0.005 N \cdot m^{-2}$ are 22.73% and 27.27%.
324 For the sensible heat fluxes (Fig. 8h), the probabilities of bias by Li and MM5 within $\pm 2.5 W \cdot m^{-2}$ are both 36.36%.

325 Mean bias (MB), normalized mean bias (NMB), normalized mean error (NME) and root mean square error (RMES) of
326 Li and MM5 were calculated to test the two schemes. Table 2 shows that the Li scheme generally estimates better than the

MM5 scheme. In the whole haze process, the Li scheme underestimates the momentum fluxes by 3.63% relative to the observations, while the MM5 scheme overestimates by 34.03%. The Li and MM5 schemes underestimate the sensible heat fluxes by 15.69% and 50.22%, respectively. In the three stages, the Li scheme performs much better than the MM5 scheme in the stage 1 and stage 2, especially in stage 2 when atmospheric stratification transforms from unstable to stable condition, the difference between the Li and MM5 schemes are particularly significant. The Li and MM5 schemes overestimate the momentum fluxes by 7.68% and 45.56%, respectively, while Li and MM5 underestimate the sensible heat fluxes by 33.84% and 76.88%. The error of Li is much less than that of MM5. Considering the importance of atmospheric stratification in the generation and accumulation of PM_{2.5} in stage 2, the Li scheme is expected to show better performance in online simulation of PM_{2.5} than MM5.

Based on the good behavior of the Li scheme in Gucheng, the same experiment was performed at Beijing station to discuss the effect of different land-cover types on flux calculation for two schemes. For Beijing station, the assumption $z_{om} = 1 \text{ m}$, $z_{om}/z_{oh} = 10^6$ was made to represent the surface condition of megacity due to a lack in situ measurements of surface turbulent flux. As shown in Fig. 9, the evolution of PM_{2.5} concentration at Beijing station was also divided into three stages (stage 1: 13~15; stage 2: 17~19; stage 3: 20~21) just like Gucheng in the discussion. Compare to Fig. 7, there is a significant increase in the difference of momentum and sensible heat fluxes between Li and MM5 in Fig. 9. To be specific, the momentum transfer in Beijing is obviously larger than that in Gucheng due to the great increase of the urban aerodynamic roughness length (z_{om}). In the meanwhile, the difference between Li and MM5 has a further expansion at Beijing station compared with Gucheng. The sensible heat transfer by the Li scheme has great difference between clear days and pollution days, which is, the sensible heat transfer changes acutely in the stage 1 while it changes smoothly in the stage 2 and stage 3. The sensible heat transfer by the MM5 scheme is significantly different compared with Li result due to MM5 ignored the z_{om} effect, and the small number of z_{oh} keeps the sensible heat fluxes at a low level in all three stages.

To quantify the differences between the two schemes, a relative difference is defined in percentage:

$$\Delta V = \left| \frac{V_{Li} - V_{MM5}}{V_{MM5}} \right| \times 100 \%, \quad (21)$$

where V_{Li} and V_{MM5} are the momentum (or sensible heat) flux calculated by the Li and MM5 schemes, respectively. We obtained the relative differences at the two stations in the three stages through the statistics. It is clearly that the largest relative difference at Gucheng station is in the stage 2 and the value at Beijing station is in the stage 1. The differences in Beijing are always larger than that in Gucheng for each three stages. Specifically, the relative difference of momentum flux in stage 1, stage 2 and stage 3 increases by 73%, 34% and 27%, respectively, and the results of sensible heat flux are 289%, 52% and 68%, respectively.

We further tested the two schemes in whole Jing-Jin-Ji region. Figure 10 shows the mean momentum and sensible heat fluxes calculated by Li and MM5 schemes and their difference in Jing-Jin-Ji during the pollution episode. The

358 assumption $z_{0m} = 0.1$ m, $z_{0m}/z_{0h} = 10^3$ were used to represent the average condition of the underlying surface of
359 Jing-Jin-Ji region. As shown in Fig. 10, the momentum fluxes calculated by Li are less than that by MM5 in most stations;
360 the sensible heat fluxes calculated by Li are usually larger than that by MM5. The result is consistent with the experiment of
361 Gucheng station, which further indicates the importance of considering z_{0m} and z_{0h} at the same time.

362 5 Conclusions

363 Using the observed momentum and sensible heat fluxes, together with conventional meteorological data including
364 pressure, temperature, humidity and wind speed from December 1, 2016 to January 9, 2017, including a severe pollution
365 episode from December 13 to 23, 2016, the differences and the performance of the two surface schemes were discussed and
366 evaluated in this paper. The evolution process of atmospheric stratification from unstable to stable corresponding to $PM_{2.5}$
367 increasing was mainly discussed. The contributions of roughness lengths (z_{0m} and z_{0h}) as well as other factors in the SL
368 schemes to the momentum and sensible heat flux calculation were also discussed in details. The results are summarized as
369 follows:

370 1) z_{0m} and z_{0h} have important effects on turbulent flux calculation in the SL schemes. Different values of z_{0m} and
371 z_{0h} in the schemes could induce great changes in the flux calculation, indicating that it is very necessary and important to
372 distinguish z_{0h} from z_{0m} . Ignoring the difference between the two in the MM5 scheme led to large errors in the calculation
373 of sensible heat fluxes and this error in Gucheng is 54%. Besides the roughness lengths, the algorithms of two schemes are
374 also one of the important factors. In addition, ignoring the effect of the RSL in schemes may also result in certain bias of
375 momentum and sensible heat fluxes in megacity regions which represent the rough underlying surface.

376 2) The effect of z_{0m}/z_{0h} on turbulent fluxes is closely related to the land-cover types (z_{0m}). A rough land-cover type
377 (large z_{0m}) should be accompanied by a large value of z_{0m}/z_{0h} . The differences of momentum and sensible heat fluxes
378 calculated by Li and MM5 were much bigger in Beijing than that in Gucheng. This suggests that the MM5 scheme probably
379 induces bigger error in megacities with rough surface (e.g., Beijing) than it in suburban area with smooth surface (e.g.,
380 Gucheng) due to the irrational algorithm of MM5 scheme itself and the ignoring difference between z_{0m} and z_{0h} .

381 3) The Li scheme generally performed better than the MM5 scheme in the calculation of both the momentum flux and
382 the sensible heat flux compared with observations at Gucheng station. The Li scheme made a better description in
383 atmospheric stratification which is closely related to the haze pollution, compared with the MM5 scheme. This advantage
384 was the most prominent in the transition stage from unstable to stable atmospheric stratification corresponding to the $PM_{2.5}$
385 accumulation. In this stage, the momentum flux calculated by Li was overestimated by 7.68% and this overestimation by
386 MM5 was up to 45.56%; the sensible heat flux by Li was underestimated by 33.84% while this underestimation by MM5
387 was even up to 76.88%. In most Jing-Jin-Ji region, the momentum fluxes calculated by Li were less than that by MM5 and

388 the sensible heat fluxes by Li were larger than that by MM5, which was consistent with Gucheng.

389 The offline study of the two SL schemes in this paper showed the superiority of the Li scheme for surface flux
390 calculation corresponding to the PM_{2.5} evolution during the haze episode in Jing-Jin-Ji in east China. The study results offer
391 the prerequisite and a possible way to improve PBL diffusion simulation and then PM_{2.5} prediction, which will be achieved
392 in the follow-up work of online integrating of the Li scheme into the atmosphere chemical model.

393 Acknowledgments

394 The study was supported by the National Key Project (2016YFC0203306, [2016YFC0203304](#)), the National (Key) Basic
395 Research and Development (973) Program of China (2014CB441201), ~~the National Key Project (2016YFC0203304)~~ [the](#)
396 [National Natural Science Foundation of China \(41505004, 41675009\)](#), and [Jiangsu Provincial Natural Science Fund Project](#)
397 [\(BK20150910\)](#).

398 References

- 399 Anurose, T. J., and Subrahmanyam, D. B.: Improvements in Sensible Heat-Flux Parametrization in the High-Resolution
400 Regional Model (HRM) Through the Modified Treatment of the Roughness Length for Heat, Bound.-Lay. Meteorol.,
401 147, 569-578, <https://doi.org/10.1007/s10546-013-9799-9>, 2013.
- 402 Ban, J., Gao, Z., and Lenschow, D. H.: Climate simulations with a new air-sea turbulent flux parameterization in the
403 National Center for Atmospheric Research Community Atmosphere Model (CAM3), *J. Geophys. Res.-Atmos.*, 115,
404 <https://doi.org/10.1029/2009JD012802>, 2010.
- 405 Beljaars, A. C. M., and Holtstag, A. A. M.: Flux parameterization over land surfaces for atmospheric models, *J. Appl.*
406 *Meteor.*, 30, 327-341, 1991.
- 407 Businger, J. A., Wyngaard, J. C., Izumi, Y., and Bradley, E. F.: Flux-profile relationships in the atmospheric surface layer, *J.*
408 *Atmos. Sci.*, 28, 181-189, 1971.
- 409 Businger, J. A.: Transfer of momentum and heat in the planetary boundary layer, *Proc. Symp. Arctic Heat Budget and*
410 *Atmospheric Circulation*, RM-5233-NSF, 305-331, 1966.
- 411 Chen, F., and Zhang, Y.: On the coupling strength between the land surface and the atmosphere: From viewpoint of surface
412 exchange coefficients, *Geophys. Res. Lett.*, 36, <https://doi.org/10.1029/2009GL037980>, 2009.
- 413 Chen, Y., Yang, K., He, J., Qin, J., Shi, J., Du, J., and He, Q.: Improving land surface temperature modeling for dry land of
414 China, *J. Geophys. Res.-Atmos.*, 116, <https://doi.org/10.1029/2011JD015921>, 2011.
- 415 Cheng, F. Y., Chin, S. C., and Liu, T. H.: The role of boundary layer schemes in meteorological and air quality simulations of
416 the Taiwan area, *Atmos. Environ.*, 54, 714-727, <https://doi.org/10.1016/j.atmosenv.2012.01.029>, 2012.

417 Cheng, Y., and Brutsaert, W.: Flux-profile relationships for wind speed and temperature in the stable atmospheric boundary
418 layer, *Bound.-Lay. Meteorol.*, 114, 519-538, <https://doi.org/10.1007/s10546-004-1425-4>, 2005.

419 De Ridder, K.: Bulk Transfer Relations for the Roughness Sublayer, *Bound.-Lay. Meteorol.*, 134, 257-267,
420 <https://doi.org/10.1007/s10546-009-9450-y>, 2010.

421 Dyer, A. J.: A review of flux-profile relationships, *Bound.-Lay. Meteorol.*, 7, 363-372, <https://doi.org/10.1007/BF00240838>,
422 1974.

423 Dyer, A. J.: The turbulent transport of heat and water vapour in an unstable atmosphere, *Quart. J. Roy. Meteor. Soc.*, 93,
424 501-508, <https://doi.org/10.1002/qj.49709339809>, 1967.

425 Florens, E., Eiff, O., and Moulin, F.: Defining the roughness sublayer and its turbulence statistics, *Exp. Fluids*, 54, 1500,
426 <https://doi.org/10.1007/s00348-013-1500-z>, 2013.

427 Garratt, J. R., and Francey, R. J.: Bulk characteristics of heat transfer in the unstable, baroclinic atmospheric boundary layer,
428 *Bound.-Lay. Meteorol.*, 15, 399-421, <https://doi.org/10.1007/BF00120603>, 1978.

429 Garratt, J. R., and Hicks, B. B.: Momentum, heat and water vapour transfer to and from natural and artificial surfaces, *Quart.*
430 *J. Roy. Meteor. Soc.*, 99, 680-687, 1973.

431 Garratt, J. R.: Transfer characteristics for a heterogeneous surface of large aerodynamic roughness, *Quart. J. Roy. Meteor.*
432 *Soc.*, 104, 491-502, 1978.

433 Högström, U.: Review of some basic characteristics of the atmospheric surface layer, *Bound.-Lay. Meteorol.*, 78, 215-246,
434 <https://doi.org/10.1007/BF00120937>, 1996.

435 Holtslag, A. A. M., and De Bruin, H. A. R.: Applied modeling of the nighttime surface energy balance over land, *J. Appl.*
436 *Meteor.*, 27, 689-704, 1988.

437 Hu, X. M., Nielsen-Gammon, J. W., and Zhang, F.: Evaluation of three planetary boundary layer schemes in the WRF model,
438 *J. Appl. Meteorol. Climatol.*, 49, 1831-1844, <https://doi.org/10.1175/2010JAMC2432.1>, 2010.

439 Jiménez, P. A., Dudhia, J., González-Rouco, J. F., Navarro, J., Montávez, J. P., and García-Bustamante, E.: A revised scheme
440 for the WRF surface layer formulation, *Mon. Wea. Rev.*, 140, 898-918, <https://doi.org/10.1175/MWR-D-11-00056.1>,
441 2012.

442 Kot, S. C., and Song, Y.: An Improvement of the Louis Scheme for the Surface Layer in an Atmospheric Modelling System,
443 *Bound.-Lay. Meteorol.*, 88, 239-254, <https://doi.org/10.1023/A:100119329423>, 1998.

444 Launiainen, J.: Derivation of the relationship between the Obukhov stability parameter and the bulk Richardson number for
445 flux-profile studie, *Bound.-Lay. Meteorol.*, 76, 165-179, <https://doi.org/10.1007/BF00710895>, 1995.

446 Li, T., Wang, H., Zhao, T., Xue, M., Wang, Y., Che, H., and Jiang, C.: The Impacts of Different PBL Schemes on the
447 Simulation of PM_{2.5} during Severe Haze Episodes in the Jing-Jin-Ji Region and Its Surroundings in China, *Adu.*
448 *Meteorol.*, <http://dx.doi.org/10.1155/2016/6295878>, 2016a.

449 Li, Y., Gao, Z., Li, D., Chen, F., Yang, Y., and Sun, L.: An Update of Non-iterative Solutions for Surface Fluxes Under
450 Unstable Conditions, *Bound.-lay. Meteorol.*, 156, 501-511, <https://doi.org/10.1007/s10546-015-0032-x>, 2015.

451 Li, Y., Gao, Z., Li, D., Chen, F., Yang, Y., and Sun, L.: Erratum to: An Update of Non-iterative Solutions for Surface Fluxes
452 Under Unstable Conditions, *Bound.-Lay. Meteorol.*, 161: 225-228, 2016b.

453 Li, Y., Gao, Z., Li, D., Wang, L., and Wang, H.: An improved non-iterative surface layer flux scheme for atmospheric stable
454 stratification conditions, *Geosci. Model Dev.*, 7, 515-529, <https://doi.org/10.5194/gmd-7-515-2014>, 2014.

455 Li, Y.: On the Surface Turbulent Fluxes Calculation in Numerical Models, Beijing: university of Chinese academy of
456 sciences, 2014.

457 Li, Z., Guo, J., Ding, A., Liao, H., Liu, J., Sun, Y., Wang, T., Xue, H., Zhang, H., and Zhu, B.: Aerosol and boundary-layer
458 interactions and impact on air quality, *Natl. Sci. Rev.*, 4, 810–833, <https://doi.org/10.1093/nsr/nwx117>, 2017.

459 Liu, T. T., Gong, S. L., He, J. J., Yu, M., Wang, Q. F., Li, H. R., Liu, W., Zhang, J., Li, L., Wang, X. G., Li, S. L., Lu, Y. L.,
460 Du, H. T., Wang, Y. Q., Zhou, C. H., Liu, H. L. and Zhao, Q. C.: Attributions of meteorological and emission factors to
461 the 2015 winter severe haze pollution episodes in China's Jing-Jin-Ji area, *Atmos. Chem. Phys.*, 17, 2971–2980,
462 <https://doi.org/10.5194/acp-17-2971-2017>, 2017.

463 Louis, J. F.: A parametric model of vertical eddy fluxes in the atmosphere. *Bound.-Lay. Meteorol.*, 17, 187-202,
464 <https://doi.org/10.1007/BF00117978>, 1979.

465 Louis, J. F., Tiedtke, M., and Geleyn, J. F.: A short history of the operational PBL parameterization at ECMWF, in Workshop
466 on Planetary Boundary Layer Parameterization, November 1981, ECMWF, Reading, U.K., pp. 59–79, 1982.

467 Monin, A. S., and Obukhov, A. M.: Basic laws of turbulent mixing in the surface layer of the atmosphere, *Contrib. Geophys.*
468 *Inst. Acad. Sci., USSR*, 24, 163–187, 1954.

469 Paulson, C. A.: The mathematical representation of wind speed and temperature profiles in the unstable atmospheric surface
470 layer, *J. Appl. Meteorol.*, 9, 857-861, 1970.

471 Sharan, M., and Srivastava, P.: A Semi-Analytical Approach for Parametrization of the Obukhov Stability Parameter in the
472 Unstable Atmospheric Surface Layer, *Bound.-Lay. Meteorol.*, 153, 339-353, <https://doi.org/10.1007/s10546-014-9948-9>,
473 2014.

474 Sicart, J. E., Litt, M., Helgason, W., Tahar, V. B., and Chaperon, T.: A study of the atmospheric surface layer and roughness
475 lengths on the high-altitude tropical Zongo glacier, Bolivia, *J. Geophys. Res.-Atmos.*, 119, 3793–3808,
476 <https://doi.org/10.1002/2013JD020615>, 2014.

477 Simpson, I. J., Thurtell, G. W., Neumann, H. H., Den Hartog, G., and Edwards, G. C.: The Validity of Similarity Theory in
478 the Roughness Sublayer Above Forests, *Bound.-Lay. Meteorol.*, 87, 69-99, <https://doi.org/10.1023/A:1000809902980>,
479 1998.

480 Stewart, J. B., Kustas, W. P., Humes, K. S., Nichols, W. D., Moran, M. S., and De Bruin, H. A. R.: Sensible heat
481 flux-radiometric surface temperature relationship for eight semiarid areas, *J. Appl. Meteorol.*, 33, 1110-1117, 1994.

482 Stull, R. B.: *An Introduction to Boundary Layer Meteorology*, Kluwer Academic Publishers, London, 1988.

483 Sugawara, H., and Narita, K.: Roughness length for heat over an urban canopy, *Theor. Appl. Climatol.*, 95, 291-299,
484 <https://doi.org/10.1007/s00704-008-0007-7>, 2009.

485 Sun, J.: Diurnal Variations of Thermal Roughness Height over a Grassland, *Bound.-Lay. Meteorol.*, 92, 407-427,
486 <https://doi.org/10.1023/A:1002071421362>, 1999.

487 Tymvios, F., Charalambous, D., Michaelides, S., and Lelieveld, J.: Intercomparison of boundary layer parameterizations for
488 summer conditions in the eastern Mediterranean island of Cyprus using the WRF-ARW model, *Atmos. Res.*, 208, 45-59,
489 <https://doi.org/10.1016/j.atmosres.2017.09.011>, 2017.

490 Vautard, R., Moran, M. D., Solazzo, E., Gilliam, R. C., Matthias, V., Bianconi, R., Chemel, C., Ferreira, J., Geyer, B.,
491 Hansen, A. B., Jericevic, A., Prank, M., Segers, A., Silver, J. D., Werhahn, J., Eolke, R., Rao, S. T., and Galmarini, S.:
492 Evaluation of the meteorological forcing used for the Air Quality Model Evaluation International Initiative (AQMEII)
493 air quality simulations, *Atmos. Environ.*, 53, 15-37, <https://doi.org/10.1016/j.atmosenv.2011.10.065>, 2012.

494 Verhoef, A., De Bruin, H. A. R., and Van Den Hurk, B. J. J. M.: Some Practical Notes on the Parameter kB-1 for Sparse
495 Vegetation., *J. Appl. Meteorol.*, 36, 560-572, 1997.

496 Wang, H., Shi, G. Y., Zhang, X. Y., Gong, S. L., Tan, S. C., Chen, B., Che, H. Z., and Li, T.: Mesoscale modeling study of the
497 interactions between aerosols and PBL meteorology during a haze episode in China Jing-Jin-Ji and its near surrounding
498 region - Part 2: Aerosols' radiative feedback effects, *Atmos. Chem. Phys.*, 15, 3277-3287,
499 <https://doi.org/10.5194/acp-15-3277-2015>, 2015b.

500 Wang, H., Tan, S. C., Wang, Y., Jiang, C., Shi, G., Zhang, M., and Che, H. Z.: A multisource observation study of the severe
501 prolonged regional haze episode over eastern China in January 2013, *Atmos. Environ.*, 89, 807-815,
502 <https://doi.org/10.1016/j.atmosenv.2014.03.004>, 2014.

503 Wang, H., Xue, M., Zhang, X. Y., Liu, H. L., Zhou, C. H., Tan, S. C., Che, H. Z., Chen, B., and Li, T.: Mesoscale modeling
504 study of the interactions between aerosols and PBL meteorology during a haze episode in China Jing-Jin-Ji and its
505 nearby surrounding region - Part 1: Aerosol distributions and meteorological features, *Atmos. Chem. Phys.*, 15,
506 3257-3275, <https://doi.org/10.5194/acp-15-3257-2015>, 2015a.

507 Wang, S., Wang, Q., and Doyle, J.: Some improvements to Louis surface flux parameterization. Paper presented at 15th
508 symposium on boundary layers and turbulence, American Meteorological Society, 15–19, 2002, Wageningen,
509 Netherlands.

510 Webb, E. K., Pearman, G. I., and Leuning, R.: Correction of flux measurements for density effects due to heat and water
511 vapour transfer, *Quart. J. Roy. Meteor. Soc.*, 106, 85-100, 1980.

512 Webb, E. K.: Profile relationships: The log-linear range, and extension to strong stability, *Quart. J. Roy. Meteor. Soc.*, 96,
513 67-90, 1970.

514 Wouters, H., De Ridder, K., and van Lipzig, N. P. M.: Comprehensive Parametrization of Surface-Layer Transfer
515 Coefficients for Use in Atmospheric Numerical Models, *Bound.-Lay. Meteorol.*, 145, 539-550,
516 <https://doi.org/10.1007/s10546-012-9744-3>, 2012.

517 Xie, B., Fung, J. C. H., Chan, A., and Lau, A.: Evaluation of nonlocal and local planetary boundary layer schemes in the
518 WRF model, *J. Geophys. Res.-Atmos.*, 117, 48-50, <https://doi.org/10.1029/2011JD017080>, 2012.

519 Yang, K., Koike, T., and Yang, D.: Surface Flux Parameterization in the Tibetan Plateau, *Bound.-Lay. Meteorol.*, 106,
520 245-262, <https://doi.org/10.1023/A:1021152407334>, 2003.

521 Yang, K., Koike, T., Ishikawa, H., Kim, J., Li, X., Liu, H., Liu, S., Ma, Y., and Wang, J.: Turbulent Flux Transfer over
522 Bare-Soil Surfaces: Characteristics and Parameterization, *J. Appl. Meteorol. Clim.*, 47, 276-290,
523 <https://doi.org/10.1175/2007jamc1547.1>, 2008.

524 Yang, K., Tamai, N., and Koike, T.: Analytical Solution of Surface Layer Similarity Equations, *J. Appl. Meteorol.*, 40,
525 1647-1653, 2001.

526 Yang, Y., Liu, X., Qu, Y., Wang, J., An, J., Zhang, Y., and Zhang, F.: Formation mechanism of continuous extreme haze
527 episodes in the megacity Beijing, China, in January 2013, *Atmos. Res.*, 155, 192–203,
528 <https://doi.org/10.1016/j.atmosres.2014.11.023>, 2015.

529 Zhang, B., Wang, Y., and Hao, J.: Simulating aerosol-radiationcloud feedbacks on meteorology and air quality over eastern
530 China under severe haze conditions in winter, *Atmos. Chem. Phys.*, 15, 2387–2404,
531 <http://doi.org/10.5194/acp-15-2387-2015>, 2015.

532 Zhang, D., and Anthes, R. A.: A high-resolution model of the planetary boundary layer—Sensitivity tests and comparisons
533 with SESAME-79 data, *J. Appl. Meteorol.*, 21, 1594-1609, 1982.

534 Zhang, R., Li, Q., and Zhang, R.: Meteorological conditions for the persistent severe fog and haze event over eastern China
535 in January 2013, *Sci. China Earth Sci.*, 57, 26–35, <https://doi.org/10.1007/s11430-013-4774-3>, 2014.

536 Zhong, J., Zhang, X., Dong, Y., Wang, Y., Liu, C., Wang, J., Zhang, Y., and Che, H.: Feedback effects of boundary-layer
537 meteorological factors on cumulative explosive growth of PM_{2.5} during winter heavy pollution episodes in Beijing
538 from 2013 to 2016, *Atmos. Chem. Phys.*, 18, 247–258, <https://doi.org/10.5194/acp-18-247-2018>, 2018.

539

540 **Table 1.** Typical values of z_{0m} corresponding to various land-cover types

z_{0m} / m	Land-cover types
5 ~ 50	Mountain (above 100m)
1 ~ 5	The center of large cities, hills or mountain area
0.1 ~ 1	Forests, the center of large towns
0.01 ~ 0.1	Flat grasslands, agricultural fields
$10^{-4} \sim 10^{-3}$	The snow surface, wide water surface, flat deserts
10^{-5}	The ice surface

541

542

543

544

Table 2. Statistics between the Li and MM5 schemes calculated turbulent flux at Gucheng station.

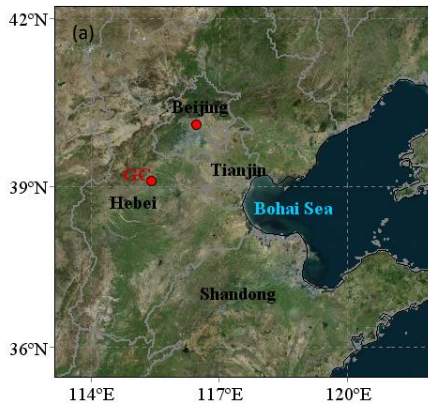
		Li				MM5			
		MB	NMB	NME	RMSE	MB	NMB	NME	RMSE
Whole	τ	-0.0006	-3.63%	54.29%	0.0142	0.0058	34.03%	63.59%	0.0143
process	H	-2.2723	-15.69%	52.73%	10.9649	-7.2735	-50.22%	69.68%	12.7946
Stage 1	τ	0.0021	9.98%	55.90%	0.0172	0.0091	43.45%	66.66%	0.0169
	H	1.1775	5.79%	37.87%	10.5734	-7.1891	-35.34%	55.70%	13.1324
Stage 2	τ	0.0013	7.68%	44.50%	0.0111	0.0079	45.56%	56.81%	0.0121
	H	-4.5752	-33.84%	50.28%	9.3995	-10.3924	-76.88%	81.40%	13.2553
Stage 3	τ	-0.0024	-13.25%	59.13%	0.0144	0.0030	16.72%	56.34%	0.0138
	H	1.2818	11.39%	66.31%	11.4778	-1.7479	-15.52%	65.90%	10.4219

545

546

547

* τ : momentum flux; H: sensible heat flux; MB: mean bias; NMB: normalized mean bias; NME: normalized mean error; RMSE: root mean square error. The units of MB and RMSE: $\mu g \cdot m^{-3}$.



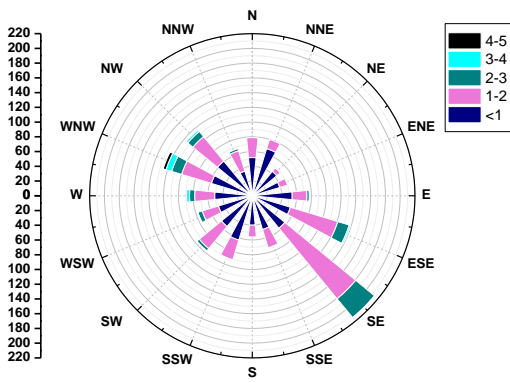
548

549 **Figure 1.** Location (a) and geographical environment (b) at Gucheng station. The map is from Bing Maps.

550

551

552



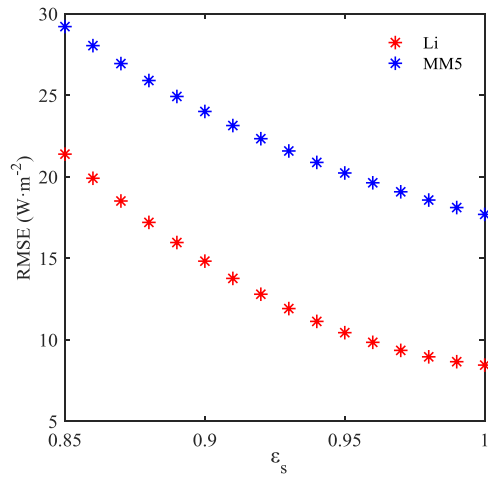
553

554 **Figure 2.** Wind Rose map at Gucheng station from December 1, 2016 to January 9, 2017.

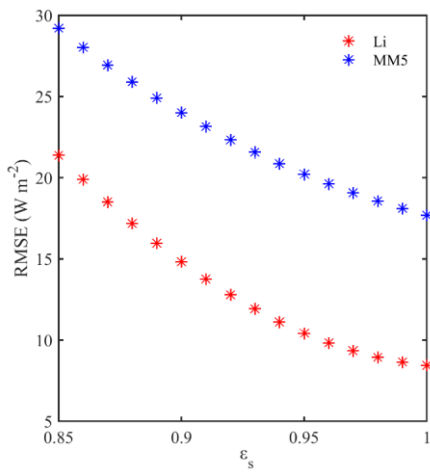
555

556

557



558



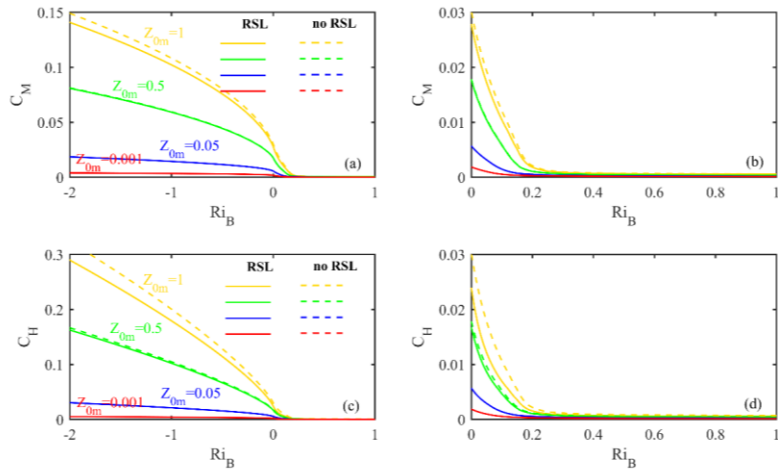
559

560 **Figure 3.** The surface emissivity ϵ_s dependence of RMSE between observed near-neutral heat fluxes and parameterized
 561 heat fluxes (red for Li and blue for MM5) at Gucheng station.

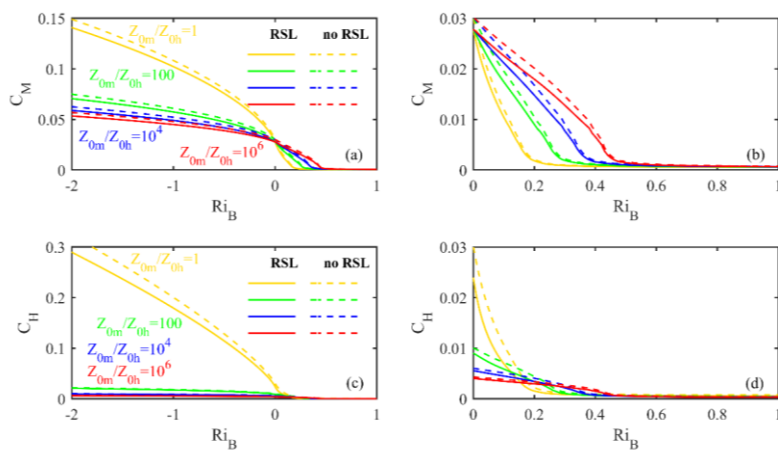
562

563

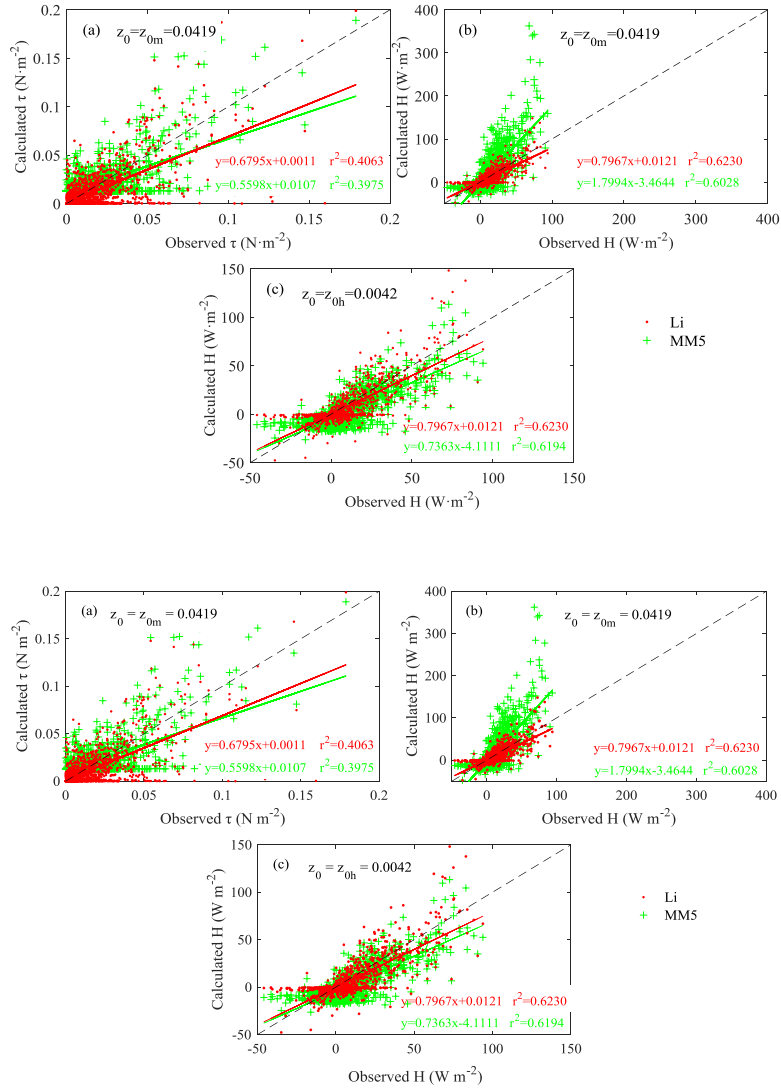
564



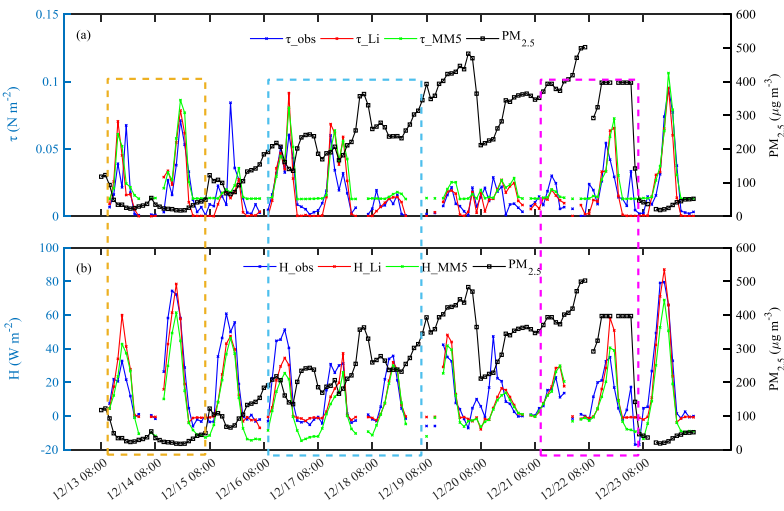
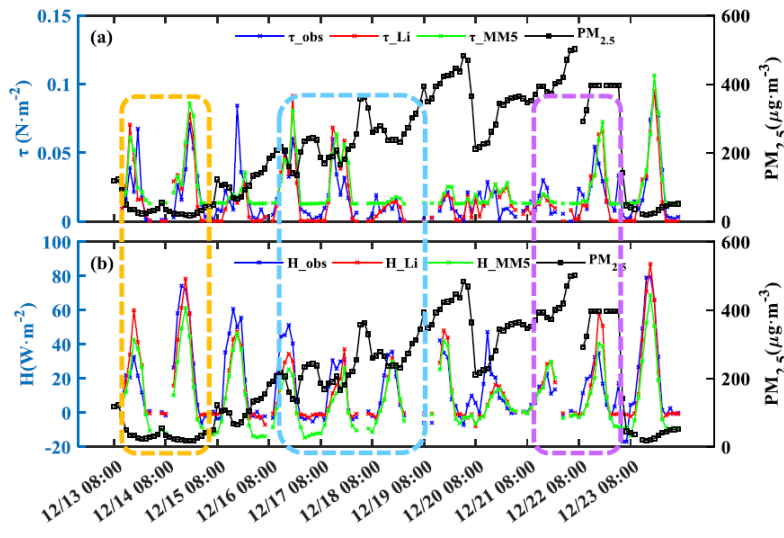
565
 566 **Figure 4.** The relationship between C_M (C_H) and Ri_B for different z_{0m} values and treatment of RSL. Solid lines:
 567 considering the RSL effect; dotted lines: without the RSL effect.
 568



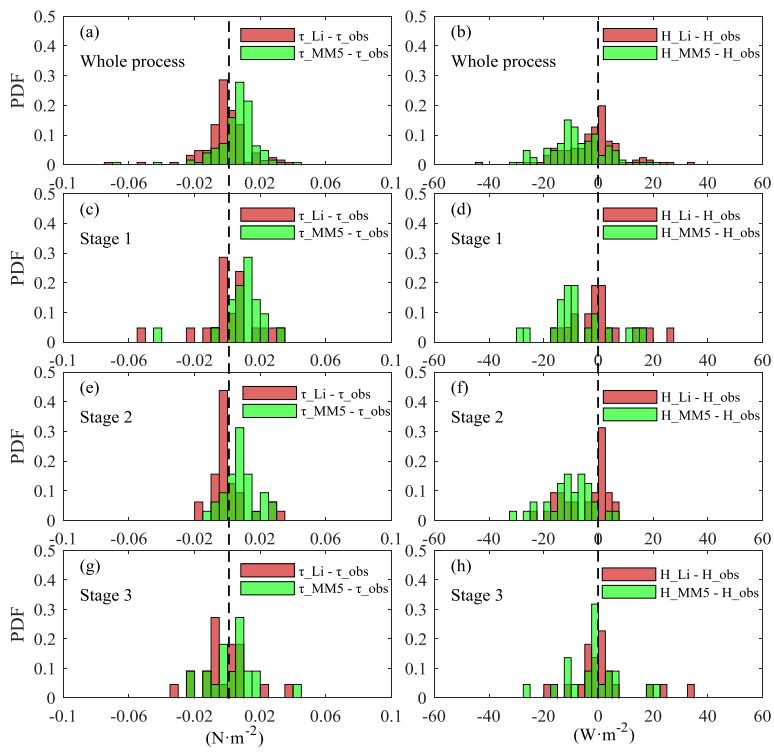
569
 570 **Figure 5.** The relationship between C_M (C_H) and Ri_B for different ratios of z_{0m} to z_{0h} and treatment of RSL. Solid lines:
 571 considering the RSL effect; dotted lines: without the RSL effect.
 572
 573
 574

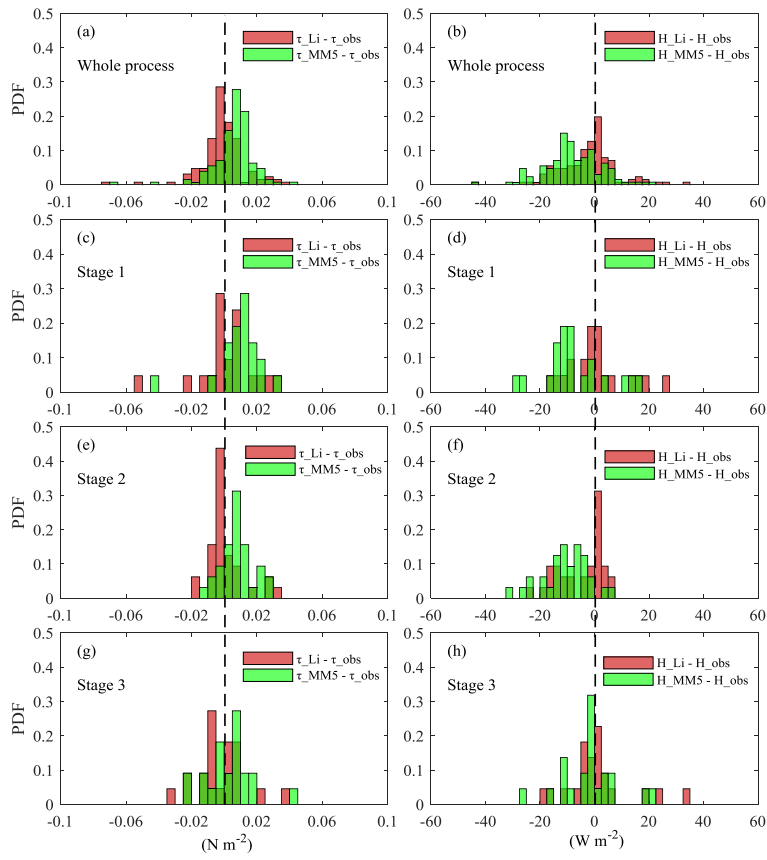


577 **Figure 6.** Comparison of calculated and observed fluxes at Gucheng station from December 1, 2016 to January 9, 2017. (a)
 578 Momentum fluxes (MM5: $z_0 = 0.0419$); (b) sensible heat fluxes (MM5: $z_0 = 0.0419$); (c) sensible heat fluxes (MM5:
 579 $z_0 = 0.0042$). Red dots: the Li scheme; green plus signs: the MM5 scheme.



585 **Figure 7.** Variations of hourly turbulent fluxes and observed $PM_{2.5}$ at Gucheng station in daytime. (a) Momentum fluxes τ
 586 (blue line: observations; red line: the Li scheme; green line: the MM5 scheme) and $PM_{2.5}$ concentration (black line); (b)
 587 sensible heat fluxes H (the same as τ) and $PM_{2.5}$ concentration (black line). Yellow box: stage 1; blue box: stage 2; purple
 588 box: stage 3.





592

593 **Figure 8.** Probability distribution functions (PDF) of the difference between calculated fluxes (momentum fluxes: left;
 594 sensible heat fluxes: right) by using two schemes (the Li scheme: red bars; the MM5 scheme: green bars) and observations in
 595 different stages (a-b: whole process; c-d: stage 1; e-f: stage 2; g-h: stage 3).

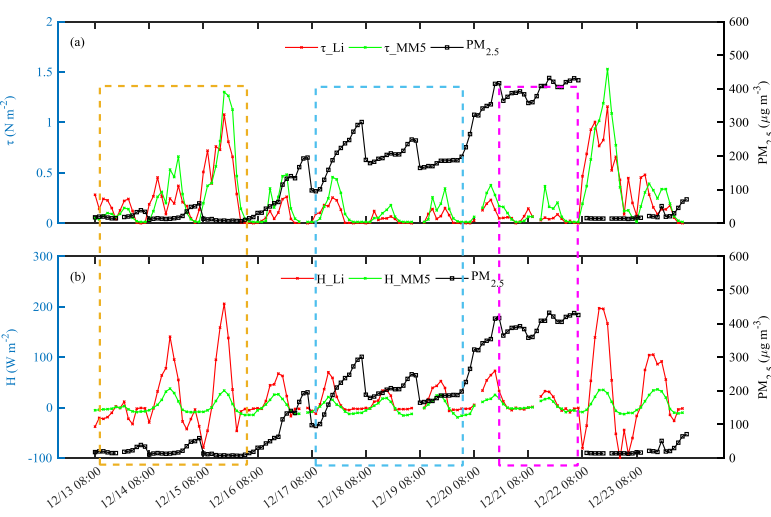
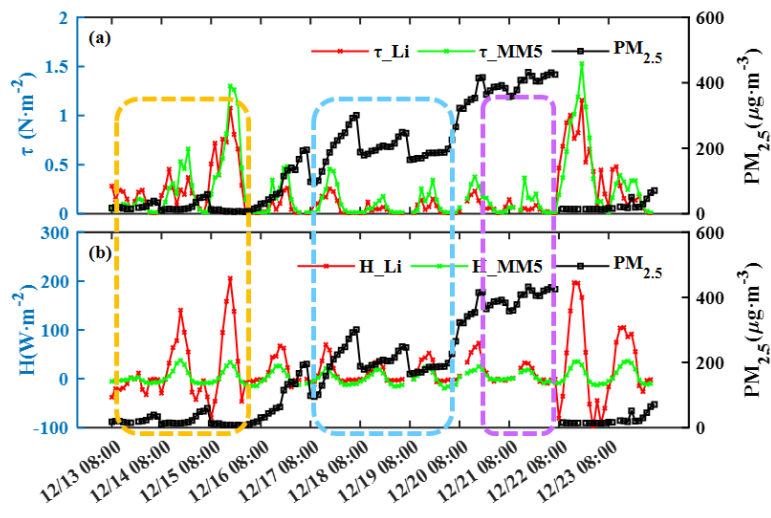
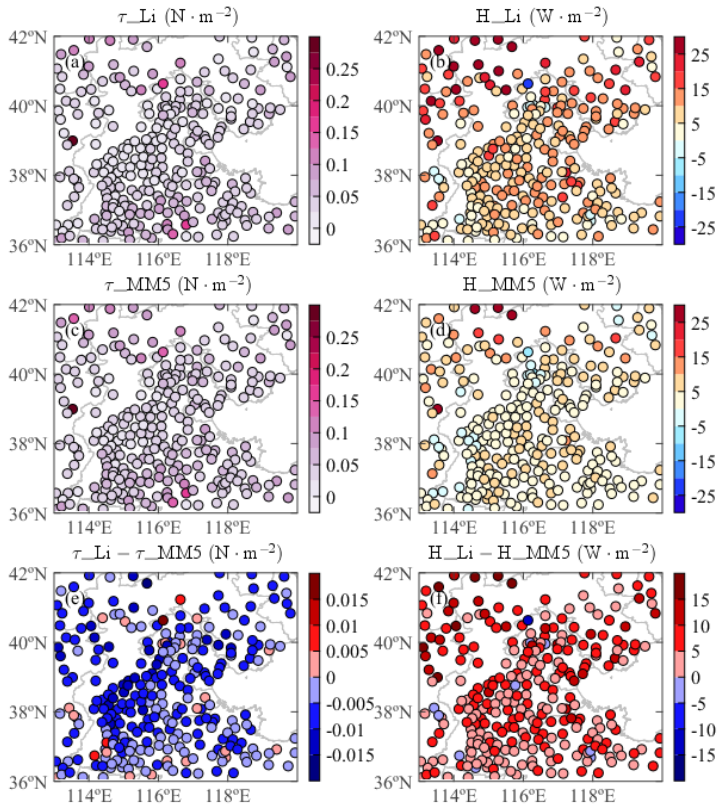
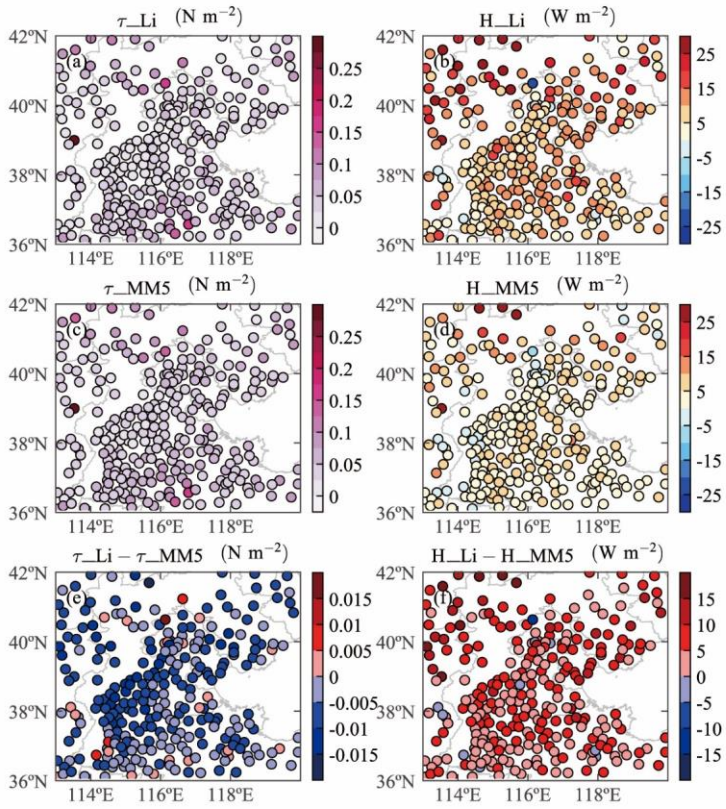


Figure 9. As in Fig. 7 but for Beijing station.



500



601

602 **Figure 10.** The mean momentum and sensible heat fluxes calculated by using two schemes (a-b: the Li scheme; c-d: the
 603 MM5 scheme) and their difference (e: difference of the momentum fluxes; f: difference of the sensible heat fluxes) in
 604 Jing-Jin-Ji during the haze episode (December 13 to 23, 2016).